Validation of a Reduced Order Model for Modular Multilevel Converters and Analysis of Circulating Current

Andres M. Lopez*, Daniel E. Quevedo*, Ricardo Aguilera†,
Tobias Geyer‡ and Nikolaos Oikonomou‡
* The University of Paderborn, Paderborn, Germany.
† The University of New South Wales, Sydney, Australia.
‡ ABB Corporate Research, Baden-Dättwil, Switzerland.
Emails: andres.lopez@upb.de, dquevedo@ieee.org, raguilera@ieee.org,
{tobias.geyer, nikolaos.oikonomou}@ch.abb.com

Abstract

In this paper, a recently proposed reduced order model for Modular Multilevel Converters is validated and used to analyze the role of the circulating current in the power transfer inside the converter. This model simplifies the analysis of the converter by removing the discontinuities and reducing the order of the system. Therefore, continuous analytical expressions can be obtained and analyzed. The reduced order is used to model the dynamics of the state space variables of the converter. The results show that, the higher the number of modules used in the converter, the more accurate are the results of the model. Moreover, the influence of different harmonic components of the circulating current over the module's voltage ripple, and the influence of the circulating current components on the power transfer in the converter are analyzed. Inter alia, the analysis shows the importance of the even order harmonics of the circulating current in the reactive power transfer within the converter.

1 Introduction

The Modular Multilevel Converter (MMC) uses low internal voltage components to handle higher external voltages. Thus, it is capable to produce high power with low distortion, giving it advantages when compared to other topologies, and making it suitable for new applications [1–3].

Each module in a MMC can be controlled independently by either inserting the module in the main branch of the converter, or removing it. Since this class of converters usually contains five or ten modules per arm, its modeling and analysis becomes a highly complex task [4, 5]. In our recent work [6], a reduced order model that approximates the discontinuities of the converter and reduces the number of control and state space variables was proposed. This model allows one to obtain explicit analytical expressions that describe the behavior of the converter variables. This reduced order model also gives one the possibility to approximate the control function (number of modules inserted) by a continuous value. The first purpose of the current paper is to analyze the effects of this approximation on the accuracy of the model, thereby showing the good model performance at a relatively low number of modules.

The circulating current in an MMC flows trough the converter without going out to the load. This gives the possibility to manipulate this current without strongly affecting the output variables [7–12]. In [13, 14], the value of the circulating current is set to a DC value, which is the minimum requirement for power transfer from the input to the output. However, in [6, 15], it is demonstrated that the addition of harmonic components can be used to reduce the ripple in the modules of the converter, giving the possibility to use smaller capacitors. Although harmonics are always injected into the circulating current, there is also the possibility to inject the harmonics in the load current. This can reduce even further the voltage ripple in the modules of the converter. This motivates the second purpose of this paper, namely to analyze the injection of harmonic components in both currents, showing which components should be injected. An analysis of the influence of the circulating current on the power transfer inside the converter

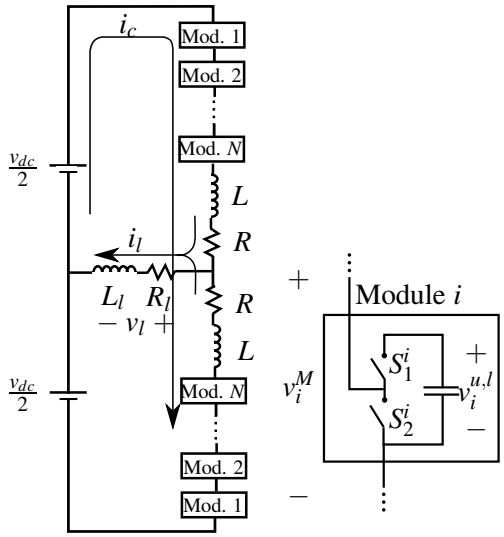

Figure 1: Typical single-phase MMC configuration with N modules per arm. v_{dc} is the DC input voltage and v_l demarks the voltage of the load (output)

is also presented. This analysis illustrates the importance of this current in the reactive power transfer between the arms of the converter, and gives insight into the role of this particular current.

The remaining paper is organized as follows: Section II presents the MMC. Section III revises the reduced order model proposed in [6]. Section IV analyzes the quantization effects on the reduced order model. Section V analyzes the effect of the harmonic components on the currents of the converter. Finally, Section VI shows the influence of the circulating current on the power transfer inside the converter. Section VII draws conclusions.

2 Modular multilevel converter (MMC)

The MMC is a power converter topology which transforms an electrical waveform from DC to AC. For each AC phase (see Fig. 1), this is accomplished by two arms inserted between the upper and the lower DC-link rail, with the center tap being the phase terminal. Each branch consists of the series-connection of N modules. Each module consists of two semiconductor switches and one capacitor. The present work focuses on a single phase MMC shown in Fig. 1.

In order to control the MMC, the switch positions of each module can be chosen independently to one of two possible positions as shown in Table I. A module is considered "inserted" when its voltage (v_i^M) is equal to the voltage of its respective capacitor.

Using basic electrical circuit analysis methods, an MMC (Fig. 1) with N submodules per arm can be described by the following state space model

$$\frac{d\vec{x}(t)}{dt} = \mathcal{A}\left(\vec{\mu}^u(t), \vec{\mu}^l(t)\right)\vec{x}(t) + \mathcal{B}v_{dc} \tag{1}$$

$$\vec{x}(t) \triangleq \begin{bmatrix} i_c(t) & i_l(t) & v_1^u(t) & \cdots & v_N^u(t) & v_1^l(t) & \cdots & v_N^l(t) \end{bmatrix}^T \tag{2}$$

Here, i_c and i_l stand for the circulating and load current respectively; v_i^u and v_i^l represent the capacitor voltages on the module i of upper (u) and lower (l) arms.

In (1), $\vec{\mu}^u(t)$ and $\vec{\mu}^l(t)$ represent the control signals for each module on the upper and lower arms. The components of these control signals can take the value of 1 (module inserted) or 0 (module not inserted) and are defined as follows

$$\vec{\mu}^u(t) \triangleq \begin{bmatrix} \mu_1^u(t) & \cdots & \mu_N^u(t) \end{bmatrix}^T,\ \mu_i^u(t) \in \{0,1\} \tag{3}$$

Table I: Switch positions

S_1^i	S_2^i	v_i^M
ON	OFF	v_i^C
OFF	ON	0
ON	ON	n.a.
OFF	OFF	n.a.

$$\vec{\mu}^l(t) \triangleq \begin{bmatrix}\mu_1^l(t) & \cdots & \mu_N^l(t)\end{bmatrix}^T, \mu_l^u(t) \in \{0,1\} \tag{4}$$

Expressions for the state space matrices $\mathcal{A}\left(\vec{\mu}^u(t),\vec{\mu}^l(t)\right)$ and $\mathcal{B}$ can be found in [6].

3 Reduced order model and accuracy

In [6] a reduced order model for MMCs was recently proposed. This model aims to simplify the analysis of the MMC by reducing the number of state space variables and giving the possibility to remove the discontinuities stemming from the switching signals. This section briefly revises the reduced order model, a detailed description can be found in [6]. The model is obtained by assuming that the capacitor voltages are balanced[1]:

$$v_i^u(t) = v_j^u(t) = v^u(t), \quad \forall i,j \in \{1,2,\ldots,N\} \tag{5}$$

$$v_i^l(t) = v_j^l(t) = v^l(t), \quad \forall i,j \in \{1,2,\ldots,N\} \tag{6}$$

Given (5) and (6) the MMC model (1) can be reduced as follows:

$$\dot{\vec{x}}(t) = A\left(\mu^u(t),\mu^l(t)\right)\vec{x}(t) + Bv_{dc}, \tag{7}$$

$$A\left(\mu^u(t),\mu^l(t)\right) \triangleq \begin{bmatrix} -\frac{R}{L} & 0 & -\frac{1}{2L}\mu^u(t) & -\frac{1}{2L}\mu^l(t) \\ 0 & -\frac{R+2R_l}{L+2L_l} & -\frac{1}{L+2L_l}\mu^u(t) & \frac{1}{L+2L_l}\mu^l(t) \\ \frac{1}{NC}\mu^u(t) & \frac{1}{2NC}\mu^u(t) & 0 & 0 \\ \frac{1}{NC}\mu^l(t) & -\frac{1}{2NC}\mu^l(t) & 0 & 0 \end{bmatrix} \tag{8}$$

$$\vec{x}(t) \triangleq \begin{bmatrix} i_c(t) & i_l(t) & v^u(t) & v^l(t)\end{bmatrix}^T \tag{9}$$

$$B \triangleq \begin{bmatrix}\frac{1}{2L} & 0 & 0 & 0\end{bmatrix}^T. \tag{10}$$

In the above,

$$\mu^u(t) \triangleq \sum_{j=1}^{N}\mu_j^u(t), \quad \mu^u(t) \in \{0,\ldots,N\} \tag{11}$$

$$\mu^l(t) \triangleq \sum_{j=1}^{N}\mu_j^l(t), \quad \mu^l(t) \in \{0,\ldots,N\} \tag{12}$$

are the modulation functions. The response of the reduced order model is compared with the converter response using the following goodness of FIT measure (coefficient of determination R^2 [16])

$$FIT = \left(1 - \frac{\|\hat{y}-y\|^2}{\|y-\bar{y}\|^2}\right)100\% \tag{13}$$

[1]Note that $v^u = v^l$ is not imposed.

where y is the response of the full order model, $\hat{y}$ the response of the reduced order model, $\bar{y}$ the mean value of y and $\|\cdot\|$ represents the Euclidean norm of the respective vector. The closer the reduced order model is to the full order model the closer FIT is to 100%.

When (11) and (12) (quantized signals) and a voltage balancing technique are used, the FIT is greater than 99% for all the tested cases showing the good accuracy of the reduced order model.

4 Quantization effects

The reduced order model, presented in Section III, reduces the number of control inputs to two ((11) and (12)), independent of the number of modules used. These inputs include the quantization effect of the original inputs. To ease the analysis of the system, the control signal can be approximated by a function without discontinuities. This is important since, provided the model is accurate, it opens the door to new analysis and design based on the continuous reduced order dynamical model.

In order to test the accuracy of the proposed reduced order model of the previous section using the continuous approximation of the control signal, the waveforms of the output current, circulating current and capacitor voltages obtained with this model are compared with the waveforms obtained in simulation using the full order model. The reduced order model presupposes balanced voltages in all the modules. Therefore, a simple sorting algorithm to balance the voltages of the capacitors is used in the simulations.

To evaluate the performance of the reduced order model, sinusoidal modulation functions of the following form are used:

$$\mu^u(t) = N\frac{1+sin(\omega_0 t)}{2} \tag{14}$$

$$\mu^l(t) = N\frac{1-sin(\omega_0 t)}{2} \tag{15}$$

The model is tested with different load values. The output current is fixed at 1 p.u, whereas the time constant $\tau = L_l/R_l$ is set to different values. The simulated steady state waveforms of the reduced order model are compared with the waveforms of the full order model using the FIT measure. Fig. 2 shows the FIT index for important variables in the circuit, namely circulating current, load current, and module voltage. An additional variable that averages the FIT of the three variables is also shown. In this case, $\tau = 0.1ms$ is used, this represents a load that is mostly resistive. The results show that for a low number of modules the FIT is lower than for a greater number of modules; for more than 7 modules per arm the FIT goes higher than 90%, which can be considered a very good match between the two models.

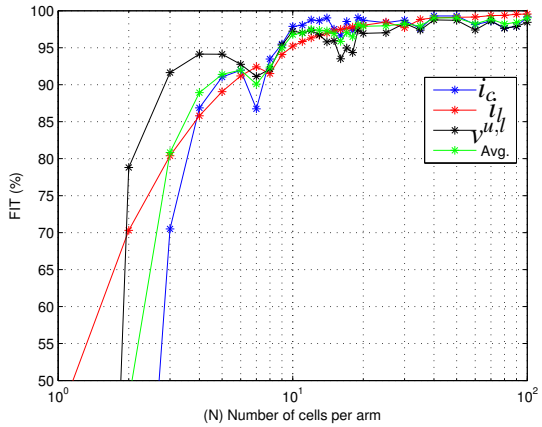

Figure 2: FIT index of the response of the reduced order model for different number of modules per arm with $\tau = 0.1m$. Avg. represents the average of the FIT of the circulating current, load current, and the module voltage.

Fig. 3 documents simulation studies with a time constant $\tau = 50m$. As in the previous case, the higher the number of levels, the higher the FIT. It can be seen that in particular i_l behaves differently from the case of Fig. 2, producing a significant lower FIT for reduced number of levels in comparison with the results obtained with a higher τ. For the other values of $\tau \in (0.5, 5, 50)$ the results are similar to Fig. 3.

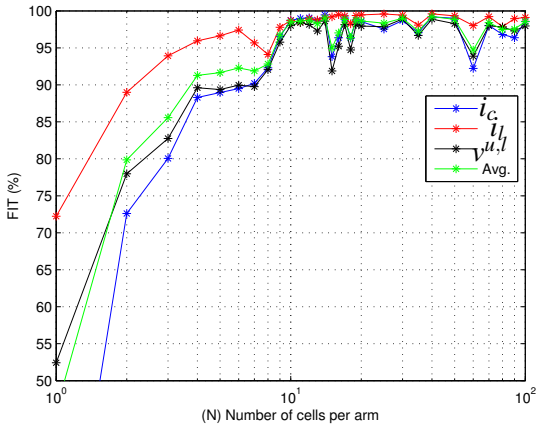

Figure 3: FIT index of the response of the reduced order model for different number of modules per arm with $\tau = 50m$. Avg. represents the average of the FIT of all the variables, circulating current, load current, and the module voltage.

Fig. 4 shows the average values of the FIT of the circulating current, load current and module voltage for all the tested cases ($\tau = 0.1m$, $50m$, 0.5, 5, 50). Here one can clearly observe that a larger time constants τ or a higher number of modules yields a better FIT. This comes from the fact that a larger time constant filters better the quantization noise in the load current, making it less significant and therefore producing better results. Moreover, a higher number of modules reduces the quantization noise making the approximation with soft modulation functions more accurate.

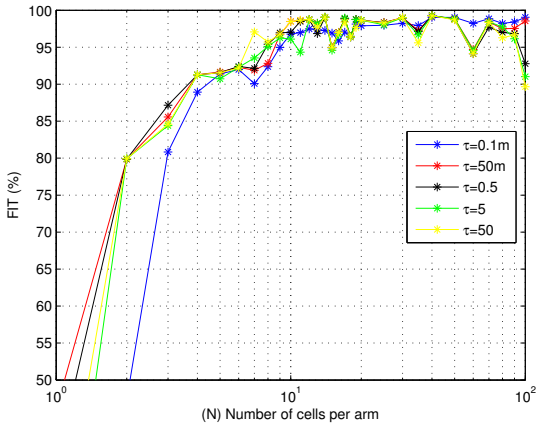

Figure 4: Comparison of the average FIT obtained with different values of τ.

5 Effect of harmonic components on the voltage ripple

Even and odd harmonics can be included in the arm currents of the converter by means of an external control loop. This allows one to have some degree of control over the behavior of the voltage ripple in the capacitors [6]. However, different harmonics (odd or even) can have different effects on the voltage ripple depending on whether they appear in the circulating or in the load current. In general a pure

sinusoidal load current is desired. However, to not limit the analysis, the effects of additional harmonics in this current are also investigated.

This section uses the reduced order model to analyze the effect each harmonic component has on the voltage ripple and concludes which harmonics should be used in order to adequately control the voltage ripple in the capacitors of the converter.

Let us assume that the load current (i_l), as shown in Fig. 1, is divided evenly between the converter upper and lower arms. Therefore, the current in the upper arm (i^u) and in the lower arm (i^l) can be written in terms of i_c and i_l and used to write the derivatives of the capacitor voltages as follows

$$\frac{dv^u(t)}{dt} = \underbrace{\left(i_c(t) + \frac{i_l(t)}{2}\right)}_{i^u} \frac{\mu^u(t)}{CN} \tag{16}$$

$$\frac{dv^l(t)}{dt} = \underbrace{\left(i_c(t) - \frac{i_l(t)}{2}\right)}_{i^l} \frac{\mu^l(t)}{CN} \tag{17}$$

Let us now assume that the voltage waveform is the same in both arms but with a phase shift ϕ_v (i.e $v^u(t) = v^l(t - \frac{\phi_v}{\omega_0})$). This assumption allows one to have evenly distributed switching losses in both arms. Using this assumption and eqs. (16) and (17) the following expression can be obtained

$$\underbrace{\left(i_c(t) + \frac{i_l(t)}{2}\right)}_{A} \underbrace{\frac{\mu^u(t)}{CN}}_{B} = \underbrace{\left(i_c(t - \frac{\phi_v}{\omega_0}) - \frac{i_l(t - \frac{\phi_v}{\omega_0})}{2}\right)}_{C} \underbrace{\frac{\mu^l(t - \frac{\phi_v}{\omega_0})}{CN}}_{D} \tag{18}$$

It is possible to analyse the problem $AB = CD$ as two separate problems $A = C$ and $B = D$. Note that $A = i^u(t)$ and $C = i^l(t - \frac{\phi_v}{\omega_0})$

In order to show $A = C$, let the circulating and load current contain additional harmonic components, as per:

$$i_c(t) = i_0 + \hat{i}_k \cos(k\omega_0 t + \phi_k),\ k \in \mathbb{N} \text{ and } k \geq 2 \tag{19}$$

$$i_l(t) = \hat{i}_l \cos(\omega_0 t + \phi) + \hat{i}_n \cos(n\omega_0 t + \phi_n),\ n \in \mathbb{N} \text{ and } n \geq 2. \tag{20}$$

The circulating current contains a $k-th$ order harmonic and the load current an $n-th$ order harmonic.

The expressions for the currents in the upper and lower arms can be written using (19) and (20) as follows

$$i^u(t) = i_c(t) + \frac{i_l(t)}{2} = i_0 + \hat{i}_k \cos(k_0 t + \phi_k) + \frac{\hat{i}_l}{2} \cos(\omega_0 t + \phi) + \frac{\hat{i}_n}{2} \cos(n\omega_0 t + \phi_n) \tag{21}$$

$$i^l(t) = i_c(t) - \frac{i_l(t)}{2} = i_0 + \hat{i}_k \cos(k\omega_0 t + \phi_k) - \frac{\hat{i}_l}{2} \cos(\omega_0 t + \phi) - \frac{\hat{i}_n}{2} \cos(n\omega_0 t + \phi_n) \tag{22}$$

Therefore, the phase shifted version of the lower arm current can be written as:

$$i^l\left(t - \frac{\phi_v}{\omega_0}\right) = i_0 + \hat{i}_k \cos(k\omega_0 t + \phi_k - k\phi_v) - \frac{\hat{i}_l}{2} \cos(\omega_0 t + \phi - \phi_v) - \frac{\hat{i}_n}{2} \cos(n\omega_0 t + \phi_n - n\phi_v). \tag{23}$$

By expanding the trigonometric function and isolating the effect of the angle ϕ_v, it is possible to notice that the only angle ϕ_v that make $i^u(t) = i^l(-\frac{\phi_v}{\omega_0})$ possible (see eqs. (21) and (23)), is $\phi_v = \pi$. Given this and rewriting the expression, the following is obtained

$$i^l\left(t - \frac{\pi}{\omega_0}\right) = i_0 + (-1)^k \hat{i}_k \cos(k\omega_0 t + \phi_k) + \frac{\hat{i}_l}{2} \cos(\omega_0 t + \phi) + (-1)^{n+1} \frac{\hat{i}_n}{2} \cos(n\omega_0 t + \phi_n) \tag{24}$$

Therefore, $i^u(t) = i^l(-\frac{\phi_v}{\omega_0})$ holds if, and only if, k is even and n is odd with $\phi_v = \pi$. Thus, the following must also hold

$$\mu^u(t) = \mu^l\left(t - \frac{\pi}{\omega_0}\right) \tag{25}$$

In order to graphically see the impact of adding even order harmonics to $i_l(t)$ and odd order harmonics to $i_c(t)$, Figs. 5 and 6 show two examples. In Fig. 5, the effect of a second order harmonic in the load current is shown. This harmonic affects significantly the waveform of the capacitor voltage on each arm differently, producing a ripple with greater amplitude in the lower arm. On the other hand, Fig. 6 shows the effect of using a third and fifth order harmonic on the circulating current. Although, the difference on the capacitor voltage ripple is not as significant as in Fig. 5, there is still a difference between the voltage of the two arms due to the use of the odd order harmonic. These differences can affect the distribution of the power losses, stressing more certain modules than others generating faster and uneven aging.

In the cases examined, the unwanted harmonics not only reduce the voltage of one of the two arms, but also tend to increase the voltage ripple in the other arm. Therefore, if the goal is to minimize the total voltage ripple in the capacitors, then odd order harmonics in the load circulating current or even order harmonics in the load current should not be used.

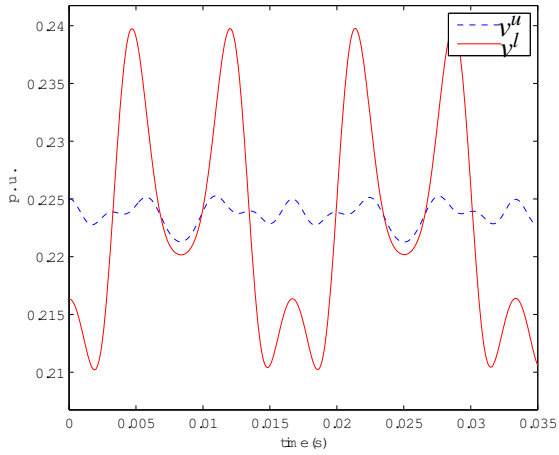

Figure 5: Capacitor voltages v_u and v_l using a second harmonic in the load current

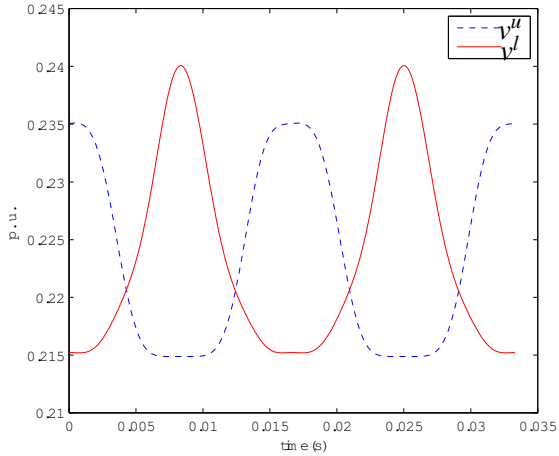

Figure 6: Capacitor voltages v_u and v_l using a third and fifth harmonic in the circulating current

6 Circulating current analysis

In order to take a deeper look at the role of circulating current in the converter, the reduced order model is used to provide simplified expressions that ease the analysis. In this section, these expressions are computed showing the role of the circulating current in the power flow in the converter. Using the reduced order model, the modulation functions for each arm can be easily obtained [6]. These modulation functions depend on the desired values of the circulating and load current, and can be written as: (see [6])

$$\mu^u(t) = \frac{1}{2v^u(t)}\left(\left(\frac{di_l(t)}{dt} + 2\frac{di_c(t)}{dt}\right)L - (i_l(t) + 2i_c(t))R + \frac{di_l(t)}{dt}L_l + 2i_l(t)R_l + v_{dc}\right) \tag{26}$$

$$\mu^l(t) = -\frac{1}{2v^l(t)}\left(\left(\frac{di_l(t)}{dt} - 2\frac{di_c(t)}{dt}\right)L - (i_l(t) - 2i_c(t))R + \frac{di_l(t)}{dt}L_l - 2i_l(t)R_l - v_{dc}\right) \tag{27}$$

The modulation functions can be used to compute the voltages of the capacitors and the power on them by multiplying the capacitor voltage and current, which can be written as:

$$P^u(t) = \frac{dE^u(t)}{dt} = \left(i_c(t) + \frac{i_l(t)}{2}\right)\frac{\mu^u(t)v^u(t)}{CN} \tag{28}$$

$$P^l(t) = \frac{dE^l(t)}{dt} = \left(i_c(t) - \frac{i_l(t)}{2}\right)\frac{\mu^l(t)v^l(t)}{CN} \tag{29}$$

where $E^u(t)$ and $E^l(t)$ represent the energy in each capacitor in the upper and lower arm respectively. Computing the energies for the capacitors in both arms, the power difference between them can be defined as

$$P^\Delta(t) \triangleq P^u(t) - P^l(t) \tag{30}$$

This term represents the power transferred between the two arms. The total power represents the power transferred from the arms to other elements in the converter, and can be defined as

$$P^T(t) \triangleq P^u(t) + P^l(t) \tag{31}$$

Note that all the capacitor voltages in the upper and lower arm are considered to be balanced. Therefore, the total power in the upper or lower arm can be calculated by multiplying the power in the capacitor by a factor N. Using the results in (26) and (27), and computing (30) and (31) the following is obtained

$$CNP^T(t) = v_{dc}i_c(t) - 2\left(i_c(t)R + \frac{di_c(t)}{dt}L\right)i_c(t) - \left(R_l i_l(t) + \frac{di_l(t)}{dt}L_l\right)i_l(t) \tag{32}$$

$$CNP^\Delta(t) = -2\left(R_l i_l(t) + \frac{di_l(t)}{dt}L_l\right)i_c(t) + \frac{v_{dc}i_l(t)}{2} - \left(i_c(t)R + \frac{di_c(t)}{dt}L\right)i_l(t) \tag{33}$$

For simplicity let us assume that the circulating current in (19) contains only a second harmonic, and the load current in (20) contains no harmonics. The total power in (32) contains the product of $i_c(t)$ by itself, as well as the product of $i_l(t)$ by itself. The products with the DC values in this equation produce the active power, which can be written as:

$$CNP^T_{\text{active}}(t) = v_{dc}i_0 - 2Ri_0^2 - 2R\hat{i}_2^2\cos(2\omega_0 t + \phi_2)^2 - R_l\hat{i}_l^2\cos(\omega_0 t + \phi)^2 - R_l\hat{i}_l^2\cos(\omega_0 t + \phi)^2/2 \tag{34}$$

The active power contains a DC part and a second and fourth harmonic AC part produced by the square of the cosine functions. The remaining terms are reactive power, and can be written as:

$$CNP^T_{\text{reactive}}(t) = v_{dc}\hat{i}_2\cos(2\omega_0 t + \phi_2) -$$
$$4i_0\hat{i}_2\cos(2\omega_0 t + \phi_2) + 4\omega_0 L\hat{i}_2^2\sin(2\omega_0 t + \phi_2)\cos(2\omega_0 t + \phi_2) - L_l\hat{i}_l^2\sin(\omega_0 t + \phi)\cos(\omega_0 t + \phi)$$

(35)

The reactive power only contains AC terms. These terms are only second and fourth harmonics and most of them are produced by the injection of a second harmonic in the circulating current.

On the other hand, (33) contains the product between $i_c(t)$ and $i_l(t)$. Since these currents or their derivatives share no common harmonics, all the power in (33) is purely reactive and can be expressed as follows

$$\begin{aligned} CNP^{\Delta}_{\text{reactive}}(t) = &\left(\frac{v_{dc}}{2} - 2R_l i_0 - 2Ri_0\right)\hat{i}_l \cos(\omega_0 t + \phi) + \omega_0 i_0 (2L_l + L)\hat{i}_l \sin(\omega_0 t + \phi) \\ &+ \frac{\hat{i}_2}{2}\left[\omega_0(3L + 2L_l)\hat{i}_l \sin(3\omega_0 t + \phi + \phi_2) + \omega_0(L - 2L_l)\hat{i}_l \sin(\omega_0 t - \phi + \phi_2)\right. \\ &\left. - 2(R + R_l)\hat{i}_l \cos(\omega_0 t - \phi + \phi_2) - 2(R + R_l)\hat{i}_l \cos(3\omega_0 t + \phi + \phi_2)\right] \end{aligned} \tag{36}$$

This expression contains only odd order harmonics (first and third). The third order harmonic is generated by the injection of the second harmonic in the circulating current

When the voltage ripple of the capacitors is reduced, the total power fluctuation is also reduced. However, the higher the amplitude of the circulating current, the higher the peak value of the power.

It can be seen in (34), (35) and (36) that the second harmonic injected into the circulating current is presented in both, the reactive and active power. However, in the active power, this harmonic only appears due to the power losses in the resistor R, which usually can be neglected compared with the power dissipated in the load resistor (see (34)). In the reactive power in (35) and (36), the circulating current plays an important role generating most of its components. Note how the frequency components on the reactive part of the total power are only even order harmonics while in the difference ($P^{\Delta}(t)$) they are only odd order harmonics.

7 Conclusions

The present work has further investigated a recently proposed reduced order model for Modular Multilevel Converters. Careful simulation studies have shown the remarkably accuracy of the model ($FIT > 99\%$ with quantization and $FIT > 80\%$ for 4 modules or more without soft control signals). The model is then used to analyze the injection of additional harmonic components to the currents of the converter. Results show that, in order to keep the voltage of all the modules equal, only even order harmonics can be used in the circulating current. The analysis also examined the injection of harmonics in the load current, showing that odd order harmonics can also help to reduce the capacitor voltages ripple. The circulating current can be understood by analyzing the power transfer between arms.

References

[1] M. Perez, S. Bernet, J. Rodriguez, S. Kouro, and R. Lizana, "Circuit topologies, modeling, control schemes, and applications of modular multilevel converters," *Power Electronics, IEEE Transactions on*, vol. 30, pp. 4–17, Jan 2015.

[2] I. Erlich, "CEP special issue on power system control," *Control Engineering Practice*, vol. 30, no. 0, pp. 91 – 92, 2014.

[3] A. Lesnicar and R. Marquardt, "An innovative modular multilevel converter topology suitable for a wide power range," in *Power Tech Conference Proceedings, 2003 IEEE Bologna*, vol. 3, pp. 6 pp. Vol.3–, June 2003.

[4] S. Rohner, J. Weber, and S. Bernet, "Continuous model of modular multilevel converter with experimental verification," in *Energy Conversion Congress and Exposition (ECCE), 2011 IEEE*, pp. 4021–4028, 2011.

[5] U. Gnanarathna, A. Gole, and R. Jayasinghe, "Efficient modeling of modular multilevel hvdc converters (mmc) on electromagnetic transient simulation programs," *Power Delivery, IEEE Transactions on*, vol. 26, no. 1, pp. 316–324, 2011.

[6] A. Lopez, D. E. Quevedo, R. P. Aguilera, T. Geyer, and N. Oikonomou, "Reference design for predictive control of modular multilevel converters," in *Australian Control Conference (AUCC 2014)*, 2014.

[7] B. Riar, T. Geyer, and U. Madawala, "Model predictive direct current control of modular multilevel converters: Modeling, analysis, and experimental evaluation," *Power Electronics, IEEE Transactions on*, vol. 30, pp. 431–439, Jan 2015.

[8] M. Vasiladiotis, N. Cherix, and A. Rufer, "Accurate voltage ripple estimation and decoupled current control for modular multilevel converters," *Proc. of the 15th International Power Electronics and Motion Control Conference (EPE-PEMC) ECCE Europe, Novi Sad, Serbia*, 2012.

[9] K. Ilves, A. Antonopoulos, L. Harnefors, S. Norrga, L. Angquist, and H.-P. Nee, "Capacitor voltage ripple shaping in modular multilevel converters allowing for operating region extension," in *IECON 2011-37th Annual Conference on IEEE Industrial Electronics Society*, pp. 4403–4408, IEEE, 2011.

[10] R. Darus, J. Pou, G. Konstantinou, S. Ceballos, and V. Agelidis, "Circulating current control and evaluation of carrier dispositions in modular multilevel converters," in *ECCE Asia Downunder (ECCE Asia), 2013 IEEE*, pp. 332–338, June 2013.

[11] S. P. Engel and R. W. D. Doncker, "Control of the modular multi-level converter for minimized cell capacitance," in *Proceedings of the 2011 14th European Conference on Power Electronics and Applications*, 2011.

[12] J. Pou, S. Ceballos, G. Konstantinou, V. Agelidis, R. Picas, and J. Zaragoza, "Circulating current injection methods based on instantaneous information for the modular multilevel converter," *Industrial Electronics, IEEE Transactions on*, vol. PP, no. 99, pp. 1–1, 2014.

[13] J. Qin and M. Saeedifard, "Predictive control of a modular multilevel converter for a back-to-back HVDC system," *IEEE Transactions on Power Delivery*, vol. 27, no. 3, pp. 1538–1547, 2012.

[14] M. Pérez, J. Rodríguez, E. Fuentes, and F. Kammerer, "Predictive control of ac-ac modular multilevel converters," *Industrial Electronics, IEEE Transactions on*, vol. 59, no. 7, pp. 2832–2839, 2012.

[15] R. Picas, J. Pou, S. Ceballos, J. Zaragoza, G. Konstantinou, and V. Agelidis, "Optimal injection of harmonics in circulating currents of modular multilevel converters for capacitor voltage ripple minimization," in *ECCE Asia Downunder (ECCE Asia), 2013 IEEE*, pp. 318–324, June 2013.

[16] N. R. Draper and H. Smith, *Applied Regression Analysis*. Wiley-Interscience, 1998.